

1           **ASSESSMENT OF GLOBAL SOLAR RADIATION AT SELLECTED POINTS IN**  
2           **NIGERIA USING ARTIFICIAL NEURAL NETWORK MODEL (ANNM)**  
3

4  
5  
6   **ABSTRACT**

7 In this study, spatial distribution, temporal variations, annual distribution, estimation and  
8 prediction of solar radiation in Nigeria was carried out using ANNs. Levenberg-Marquardt  
9 backpropagation algorithms was used for the training of the network using solar radiation data  
10 along the years (1979-2014) belonging to the thirty-six points. The data records were divided into  
11 three portions (training, testing and validation). The network processed the available data by  
12 dividing it into three portions randomly: 70% for the training, 15% for validation and the  
13 remaining 15% for testing. Input parameters were chosen as latitude, longitude, day of the year,  
14 year while observed solar radiation was chosen as targeted data (from a processed file). The output  
15 parameter was the estimated solar radiation. The network designs were tested with root mean  
16 square error and then the most successful network (taken to be best network) which is network  
17 with less error was used to carry out the study. The hyperbolic tangent sigmoid transfer function  
18 was also used between the input and the hidden layers as activation function, while the linear  
19 transfer function was used from hidden layers to the output layer as the activation function. The  
20 performance of ANNs was validated by; estimating the difference between the annual measured  
21 and estimated values were determined using coefficient of determination ( $R^2$ ). Results revealed  
22 that the  $R^2$  result was 0.82 (82%). The result of spatial variations indicated that both wet and dry  
23 seasons have their highest concentration in North-East of Nigeria. It is pertinent to also note that  
24 the lowest concentration occurred in North-West during wet season, while the lowest occurred at  
25 the South-South and South-West of Nigeria in dry season. In addition, the lowest in dry season is  
26 about  $25W/m^2$ , while that of wet season is about  $15W/m^2$ . The agreement between the temporal  
27 and annual variation of observed and estimated solar radiation reveals that the model exhibits good  
28 performance in studying solar radiation. The model was further used to predict two years ahead of  
29 the years of study.

30   **Keywords:** Global Solar Radiation; Spatial Variation; Temporal variation; Neural Networks; Architecture,  
31 Model

32   **1. INTRODUCTION**

33 Solar radiation travels to Earth through space as discrete packets of energy. Only half of that  
34 amount, however, reaches Earth's surface [1]. The atmosphere and clouds absorb or scatter the  
35 other half of the incoming sunlight. The amount of light that reaches any particular point on the  
36 ground depends on the time of the day, the day of the year, the amount of cloud cover, and the  
37 latitude at that point [1]. Knowledge of the solar radiation is essential for many applications,  
38 including architectural design, meteorological forecasting, solar energy systems, crop growth  
39 models, conversion for electricity, sciences and technology, etc. The amount of solar radiation  
40 reaching the Earth that is used to study its distributions for essential applications can best be

41 obtained by installing pyranometer at any site, and day to day readings from the instrument give  
42 us the data. The unavailability of the instruments in many sites result to the use of atmospheric  
43 parameters at a particular location to predict the global solar radiation in that location with help  
44 of different models such as artificial neural network (ANN) model. . In Nigeria, paucity of data  
45 records has been exacerbated as a result of the difficult terrain and few number of observation  
46 stations across the country. Many researchers in several areas had used artificial neural network  
47 to study the solar radiation by looking at its distributions and predictions using atmospheric  
48 parameters. The use of ANN in MATLAB to study solar radiation variations has been done in  
49 America, Europe, North and Southern Africa, but is almost nonexistent in Nigeria. This work  
50 intends, therefore, to utilize ANN algorithm in MATLAB to model and study solar radiation  
51 across Nigeria by determining its partial variation, temporal distribution, estimation and  
52 predicting two years ahead of the years of the study.

### 53 **1.1 Review of ANN Models on Solar Radiation**

54 Tymvios [2] used back-propagation method with tangent sigmoid as the transfer function to train  
55 seven ANN models using daily values of measured sunshine duration, maximum temperature,  
56 and the month number as input parameters. Normalization method was use during training. They  
57 based their study on six years data. The model deployed two hidden layers with neurons varying  
58 between 23 and 46. The best performing ANN model was one with all inputs except the month  
59 number.

60  
61 Alawi and Hinai [3] used ANN to predict solar radiation. The model used location parameters,  
62 month, temperature, vapor pressure, relative humidity, wind speed, average of pressure and  
63 sunshine duration as inputs. The model reveals excellent performance in prediction of solar  
64 radiation with ANN.

65  
66 Mohandes [4] used data from 41 stations to study solar radiation. Data from 31 stations was used  
67 in training the neural network; the data from the other stations was used for testing of the model.  
68 The model used the following input parameters: latitude, longitude, altitude and sunshine  
69 duration for the training.

70 Mihalakakou [5] used ANN to simulate total solar radiation time series in Athens, Greece.  
71 Twelve years data measured from a location in Athens, situated at latitude  $37.97^{\circ}\text{N}$ , longitude

72 23.72°E and altitude 107 m was split into two datasets. The portion measured from 1984 to 1992  
73 was used in training and the other dataset between 1993 and 1995 was used for testing. A  
74 multilayer feed-forward neural network (FFNN) based on back-propagation algorithm was  
75 designed to predict time series of global solar radiation. The selected ANN architecture consisted  
76 of one hidden layer with 16 log-sigmoid neurons and an output layer of one linear neuron.  
77 Results showed that the differences between the predicted and actual values of total solar  
78 radiation were less than 0.2%.

79  
80 Reddy and Ranjan [6] looked at solar radiation estimation using ANN and comparison with other  
81 correlation models. They created ANN models for estimation of monthly mean daily and hourly  
82 values of global solar radiation. Solar radiation data from 13 stations spread over India were used  
83 for training and testing the ANN. The solar radiation data from eleven stations (six from South  
84 India and five North India) were used for training the neural networks, and data from the  
85 remaining two locations (one each from South India and North India) were used for testing the  
86 estimated values. The solar radiation estimations by ANN were in good agreement with the  
87 actual values. The results showed that the ANN model is capable of generating global solar  
88 radiation values at places where monitoring stations were not established.

89  
90 The estimation of solar radiation in Turkey using artificial neural networks was carried out by  
91 Sozen [7]. They used Scaled conjugate gradient (SCG), Pola-Ribiere conjugate gradient (CGP)  
92 and Levenberg-Marquardt (LM) learning algorithms. Logistic sigmoid transfer function was  
93 used. In order to train the neural network, meteorological data for three years from 17 stations;  
94 11 for training and 6 for testing were used. The maximum mean absolute percentage error was  
95 found to be less than 6.7% for the testing stations. The study state that ANN model seemed  
96 promising for evaluating solar resource values at the places where there are no monitoring  
97 stations in Turkey.

98  
99 Mubiru and Banda [8] used ANN to estimate monthly average daily global solar irradiation on a  
100 horizontal surface at four locations in Uganda based on weather station data (sunshine duration,  
101 maximum temperature, and cloud cover) and location parameters of (latitude, longitude, and  
102 altitude). Results showed good agreement between the estimated and actual values of global

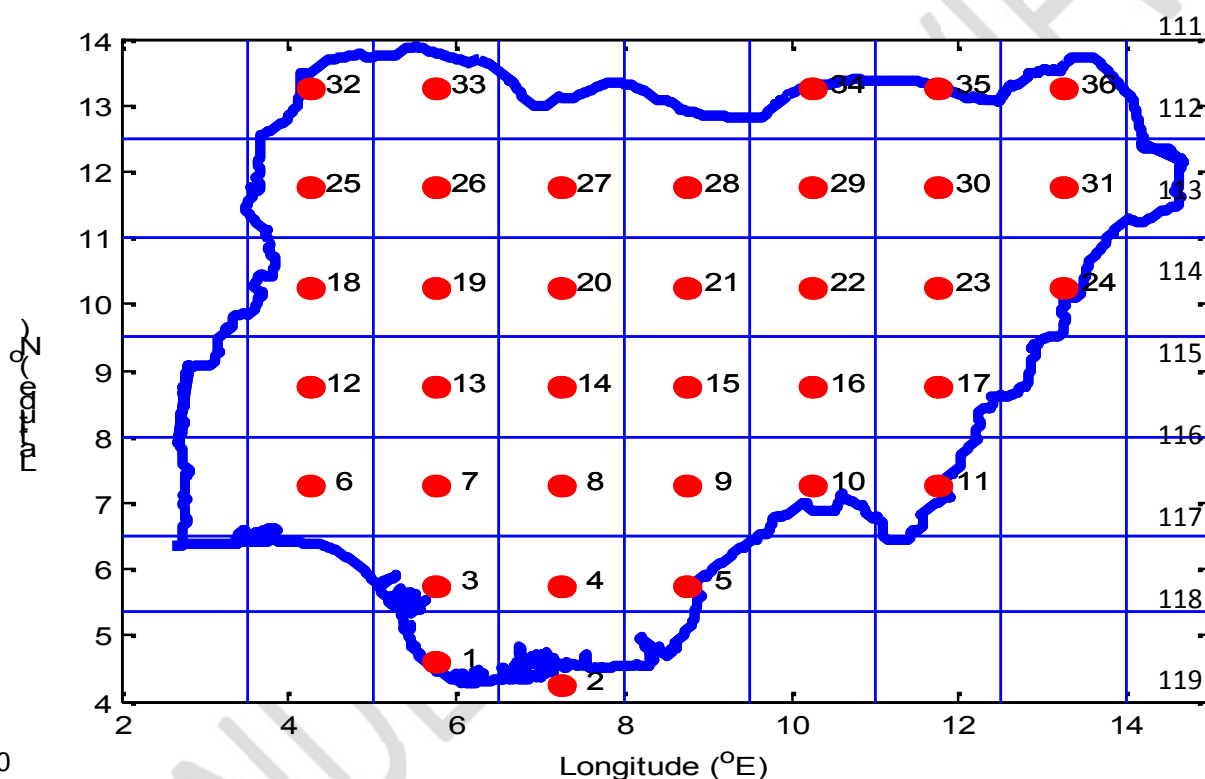
103 solar radiation. A correlation coefficient of 0.974 was obtained with MBE of 0.059 MJ/m<sup>2</sup> and  
 104 RMSE of 0.385 MJ/m<sup>2</sup>. These results confirmed the superiority of the ANN prediction model.

105 **2. Materials and Methods**

106 **2.1 The study area**

107 The study areas used in this work are thirty six (36) data points covering the spatial extent of  
 108 Nigeria as shown in Figure 1 (gridded map of selected stations in Nigeria), while Table 1 shows the  
 109 coordinates of the selected stations over Nigeria.

110



120

121 Figure 1: Gridded Map of Nigeria Showing Data Points of the selected stations in  
 122 Niger

123 Table 1: Coordinates of the selected Stations and their Data Points over Nigeria

| Points | Y Latitude<br>(°N) | X Longitude (°E) | Stations   | Local Government Area | State          |
|--------|--------------------|------------------|------------|-----------------------|----------------|
| 1      | 4.59               | 5.84             | Apoi Creek | Southern Ijaw         | Bayelsa        |
| 2      | 4.25               | 7.25             | Offshore   | Atlantic Ocean        | Atlantic Ocean |
| 3      | 5.75               | 5.75             | Ukpe Sobo  | Okpe                  | Delta          |

|    |       |       |                  |              |             |
|----|-------|-------|------------------|--------------|-------------|
| 4  | 5.75  | 7.25  | Obiohoro Osu     | Unuimo       | Imo         |
| 5  | 5.75  | 8.75  | Nsarum           | Etung        | Cross River |
| 6  | 7.25  | 4.25  | Mowo             | Isokan       | Osun State  |
| 7  | 7.25  | 5.75  | Idosale          | Ose          | Ondo State  |
| 8  | 7.25  | 7.25  | Allomo           | Ofu          | Kogi        |
| 9  | 7.25  | 8.75  | Ahile            | Gboko        | Benue       |
| 10 | 7.25  | 10.25 | Danjuma          | Ussa         | Taraba      |
| 11 | 7.25  | 11.75 | Filinga Sekenoma | Gashaka      | Taraba      |
| 12 | 8.75  | 4.25  | Alajere          | Moro         | Kwara       |
| 13 | 8.75  | 5.75  | Pategi           | Pategi       | Kwara       |
| 14 | 8.75  | 7.25  | Kabi             | Kuje         | Abuja       |
| 15 | 8.75  | 8.75  | Arugwadu         | Lafia        | Nassarawa   |
| 16 | 8.75  | 10.25 | Ibi              | Ibi          | Taraba      |
| 17 | 8.75  | 11.75 | Tainho           | Yorro        | Taraba      |
| 18 | 10.25 | 4.25  | Luma             | Borgu        | Niger       |
| 19 | 10.25 | 5.75  | Beri             | Mariga       | Niger       |
| 20 | 10.25 | 7.25  | Gwagwada         | Chikun       | Kaduna      |
| 21 | 10.25 | 8.75  | Bauda            | Lere         | Kaduna      |
| 22 | 10.25 | 10.25 | Dindima          | Bauchi       | Bauchi      |
| 23 | 10.25 | 11.75 | Pelakombo        | Bayo         | Borno       |
| 24 | 10.25 | 13.25 | Mubi             | Hong         | Adamawa     |
| 25 | 11.75 | 4.25  | Giro             | Suru         | Kebbi       |
| 26 | 11.75 | 5.75  | Bukkuyum         | Bukkuyum     | Zamfara     |
| 27 | 11.75 | 7.25  | Lugel            | Faskari      | Katsina     |
| 28 | 11.75 | 8.75  | River Armatai    | Dawakin Kudu | Kano        |
| 29 | 11.75 | 10.25 | Galadao          | Katagum      | Bauchi      |
| 30 | 11.75 | 11.75 | Damaturu         | Fune         | Yobe        |
| 31 | 11.75 | 13.25 | Dalori           | Jere         | Borno       |
| 32 | 13.25 | 4.25  | Gudu             | Gudu         | Sokoto      |
| 33 | 13.25 | 5.75  | Kadagiwa         | Wurno        | Sokoto      |
| 34 | 13.25 | 10.25 | Gunshi           | Yusufari     | Yobe        |
| 35 | 13.25 | 11.75 | Daratoshia       | Yunusari     | Yobe        |
| 36 | 13.25 | 13.25 | Abadam           | Abadam       | Borno       |

124

## 125 2.2 Designing of artificial neural network (ANN) using multilayer perceptron (MLP)

126 FFNN with MLP was used in this study. Designing, building and use of ANN multilayer  
 127 perceptron (MLP) network for simulation requires that one must follow a number of systemic  
 128 procedures. The six basics steps followed in this study include:

- 129 1. Data collection;
- 130 2. Pre-processing of data;
- 131 3. Building the network;
- 132 4. Training the network;
- 133 5. Testing the performance of the network; and

134 6. Using of the network (best network).

### 135 **2.2.1 Data Collection**

136 The solar radiations for the period 1979-2014 at the selected points were obtained from National  
137 Centers for Environmental Prediction and Climate Forecast System Reanalysis (NCEP-CSFR)  
138 under Earth System Research Laboratory, Boulder.

### 139 **2.2.2 Pre-processing data (Data extraction, sorting and file merging)**

140 The solar radiation data which was in NetCDF format were extracted and converted to binary  
141 format using panoply software, while data file merging and sorting were carried out using ferret  
142 software. The merged file contains the processed data in seven (7) columns, which compresses of  
143 year, month, day, day of the year (DOY), latitude, longitude and observed data. The interval  
144 between one point and another in the study area (Figure 1) is  $1.5^{\circ}$ , where  
145  $1^{\circ}$  represents about 111 km. The data collected were daily data, but were processed to  
146 monthly and yearly data with Microsoft excel package. The MATLAB codes was used to write the  
147 script that was used to build the neural network.

### 148 **2.2.3 Building and Training the Network**

149 In building the neural network of this study, the parameters used to build a suitable network were,  
150 network type, algorithm, network name, numbers of neurons in each layers, transfer function,  
151 weight bias, learning function, data division function and performance function. The network name  
152 used in this work was “net”, representing neural network. Feed-forward multilayer perceptron and  
153 back propagation neural network was used (from toolbox in MATHLAB version 6.5 program)  
154 because it had a better training performance and regression analysis. Figure 2 shows the schematic  
155 setup (topology) of the developed network. There are other types of networks such as nonlinear  
156 autoregressive network (NARX), autoregressive integrated moving average (ARIMA) network etc.  
157 The architecture used to build the multilayer feed-forward network comprises of three main layers;  
158 an input layer, a hidden layer and an output layer, each layer contains one or more neurons. Feed-  
159 forward networks are those in which the signal flows from the input to the output neurons, in a  
160 forward direction. The neurons on one layer are connected to those on the next layer using  
161 connections (also called weights). The neurons in the input layer act as buffers for distributing the  
162 input signals to the neurons in the hidden layer. Training and learning processes occur in the

163 hidden layer. The training process involves optimization of weights in order to minimize input-  
164 output errors. The hidden layer has a hyperbolic tangent sigmoid transfer function which acts on  
165 the input to produce the hidden weight matrix output. The output layer has a linear transfer  
166 function which act on the hidden weight matrix output to produce output matrix. Levenberg-  
167 Marquardt backpropagation algorithms were used in this study to build the network because of its  
168 high speed and efficiency in learning. This is in line with [9, 10] assertions. Buhari and Adamu  
169 [11] also observed that Levenberg-Marquardt optimization techniques has better learning rate  
170 compared to the other available functions.

171 The neural network architecture built for the training were 4-20-1, which means that we have 4  
172 neurons in the input layer, 20 neurons in the hidden layer and 1 neuron in the output layer. The  
173 inputted data through the input neurons were; year, DOY representing the time, latitude and  
174 longitude represent the coordinates. These are inputted from the processed filed out of the seven  
175 columns as the input data, with the help of the MATLAB code. The observed data were also  
176 inputted but as a targeted data. The network processes the available data during learning and  
177 training by dividing it into three portions at random: 70% for the training, 15% for validation and  
178 the remaining 15% for testing. During the training process, the weights were adjusted  
179 systematically until the simulated output was close to the observed (targeted) data of the  
180 network.

#### 181 **2.2.4 Training the network**

182 A total of 20 neural networks were trained through simulation; the difference between them is in  
183 the number of hidden layer neurons we applied (we varied the number of hidden layer neurons  
184 from 1 to 20). This is to decide an optimal number of hidden-layer neuron which is regarded as  
185 the best network. The performance of the simulation was tested using root mean square error  
186 (RMSE). There are no specific or perfect rules for deciding the most appropriate number of  
187 neurons in a hidden layer. Using an excessive number of hidden-layer neurons causes over-  
188 fitting, while a lesser number leads to under-fitting. Either scenario greatly degrades the  
189 generalization capability of the network with significant deviance in estimation and forecasting  
190 accuracy of the models [12]. Hence, according to [12] over-fitting or under-fitting is capable of  
191 leading to inaccurate estimation or forecasting if it continues. There is, therefore, a need to strike  
192 a balance such that the networks are neither under-trained nor over-trained by choosing a

193 considering apt number of hidden neurons that gave optimal values of the best or acceptable root  
 194 mean square error (RMSE).

195

196 **2.2.4.1 Modeling using Artificial Neural Networks**

197 The neural network model used in this study uses principle of optimizing weights and biases  
 198 during training. The network uses optimization method during training from input to output with  
 199 the input weight matrix, bias vector(s), hidden weight matrix and layer weight matrix  
 200 respectively. Figure 2 is the topology of the learning and training network structure which  
 201 includes input layer neurons, hidden layer neurons and output layer neurons. The input vector  
 202 elements to the desired output in Figure 2 were computed in line with [13].

203 The training sample are  $\{I, O\} = \{I_i, O_i\}$  ( $i = 1, 2, \dots, h$ ). The input vector ( $I$ ) =  $[I_{11}, I_{12}, \dots,$   
 204  $I_{1h}]$  and desired output ( $O$ ) =  $[O_{j1}, O_{j2}, \dots, O_{jh}]$ . The input matrix ( $I_m$ ) and the output matrix  
 205 ( $O_m$ ) were expressed as follows:

$$I_m = \begin{bmatrix} I_{m,1,1} & I_{m,1,2} & \dots & I_{m,1,4} \\ I_{m,2,1} & I_{m,2,2} & \dots & I_{m,2,4} \\ \vdots & \vdots & \ddots & \vdots \\ I_{m,4,1} & I_{m,4,2} & \dots & I_{m,4,4} \end{bmatrix} \quad 1$$

$$O_m = [O_{m,1,1} \quad O_{m,1,2} \quad O_{m,1,3} \quad \dots \quad O_{1,h}] \quad 2$$

208 The input vector elements enter the network through the weight matrix, that is, each element of  
 209 the input vector is connected to the weight matrix (fig.2). Then the learning machine randomly  
 210 sets the weights between the input layer and the hidden layer in the network as shown in  
 211 equation (3) and Figure (2). Again, learning machine randomly sets weights between hidden  
 212 layers to output layer in the network in form of layer weight matrix as shown in equation (4) and  
 213 Figure (2).

$$I_{wm} = \begin{bmatrix} I_{wm,1,1} & I_{wm,1,2} & \dots & I_{wm,1,4} \\ I_{wm,2,1} & I_{wm,2,2} & \dots & I_{wm,2,4} \\ \vdots & \vdots & \ddots & \vdots \\ I_{wm,h,1} & I_{wm,h,2} & \dots & I_{wm,h,4} \end{bmatrix} \quad 3$$

$$L_{wm} = [L_{wm,1,1} \quad L_{wm,1,2} \quad L_{wm,1,3} \quad \dots \quad L_{wm,1,h}] \quad 4$$

216 where h is the number of hidden layer neurons that is the dimension of hidden layer matrix . The  
 217 feed-forward neural network equations from input layer to hidden layer give the net input ( $n_1$ ) in  
 218 equation at the hidden layer and the net out ( $n_2$ ) from the hidden layer to the output layer are  
 219 shown in equations (5) and (6).



$$n_1 = I_{wm1} * I_{m1} + I_{wm2} * I_{m2} + \dots + I_{wmh} * I_{mh} + b_1 \quad 5$$

$$n_2 = L_{wm1} * H_{vm} + L_{wm2} * H_{vm} + \dots + L_{wmh,1} * H_{vm} + b_2 \quad 6$$

222 The express of equation (5) and (6) are written with MATLAB codes as equation (7) and (10) [14].  
 223 Hyperbolic tangent sigmoid transfer function ( $f_1$ ) (8) is applied to equation (7) to have hidden layer  
 224 matrix ( $H_{vm}$ ) (9). Equation (7) is the sum of the input weight matrix multiplied with input matrix plus  
 225 the bias vector one.

$$(I_{wm} * I_m + b_1) = n_1 \quad 7$$

$$f_1(n_1) = \text{tansig}(n_1) = \frac{e^{n_1} - e^{-n_1}}{e^{n_1} + e^{-n_1}} = H_{vm} \quad 8$$

$$H_{vm} = f_1(I_{wm} * I_m + b_1) \quad 9$$

229 The sum of the layer weight matrix multiplied with hidden variable matrix plus the bias vector  
 230 two gives net out ( $n_2$ ) as shown in equation (10). Linear function is applied to equation (10) as  
 231 shown in equation (11) to predict the targeted output called the output matrix as expressed in  
 232 equation (12) in the network model. The combination of equations (7 – 11) gives the straight line  
 233 equation (12) for the model that is used for the study.

$$(L_{wm} * H_{vm} + b_2) = n_2 \quad 10$$

$$f_2(n_2) = \text{purelin}(n_2) = \text{purelin}(L_{wm} * H_{vm} + b_2) = O_m \quad 11$$

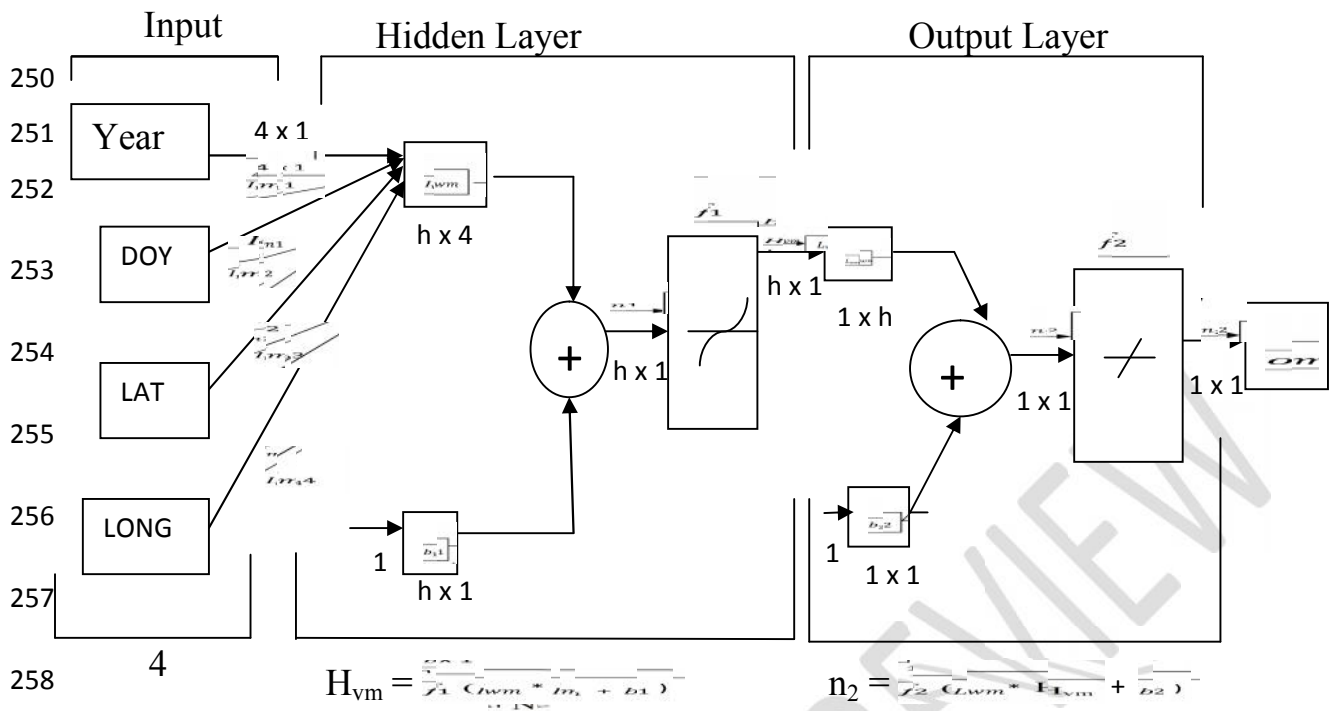
$$O_m = \text{purelin}(L_{wm} * (\text{tansig}(I_{wm} * I_m + b_1)) + b_2) \quad 12$$

237 where  $O_m$  depicts the output matrix which contains the predicted data with the network model,  
 238 while  $I_m$  depict the input matrix (year, day of the year (DOY), latitude, longitude),  $I_{wm}$   
 239 represent inputs weight matrix,  $b_1$  is bias vector one,  $H_{vm}$  is the hidden variable matrix,  $L_{wm}$  is  
 240 layer weight matrix,  $b_2$  is bias vector two,  $\text{tansig}(f_1)$  is hyperbolic tangent sigmoid transfer  
 241 function used between the input and the hidden layers as activation function, while  $\text{purelin}(f_2)$  is  
 242 the linear transfer function used from hidden layers to the output layer as the activation function.  
 243 The values of  $I_{wm}$ ,  $L_{wm}$ ,  $b_1$  and  $b_2$  of this study we be made available on request. The  
 244 application of Neural Network architecture used for building the network and training from input  
 245 to output is shown in Figure (2), while Figure (3) is the drop down window showing the neural  
 246 network training (nntraintool) process at network 20.

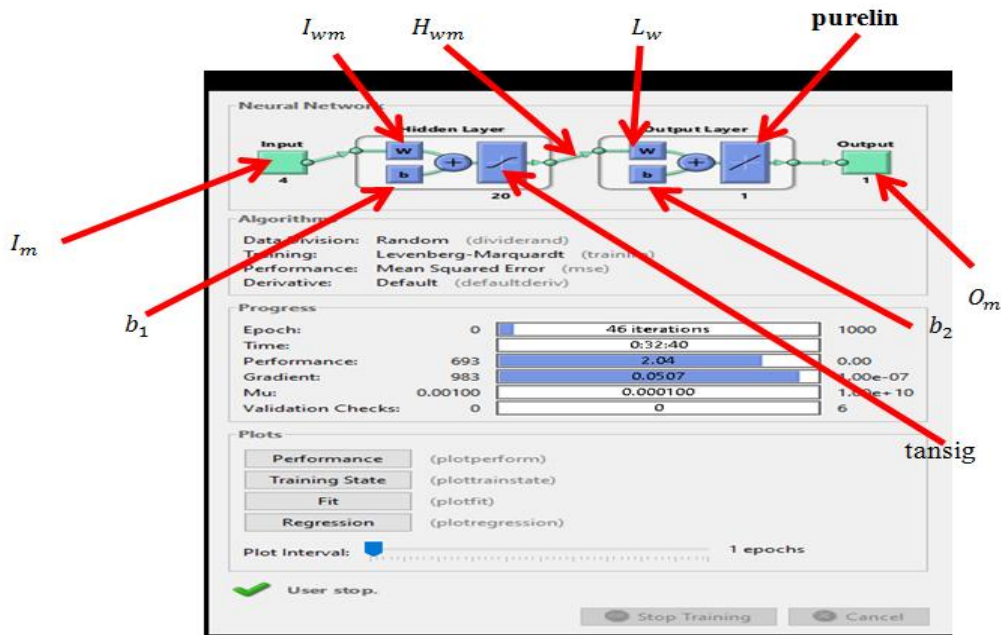
247

248

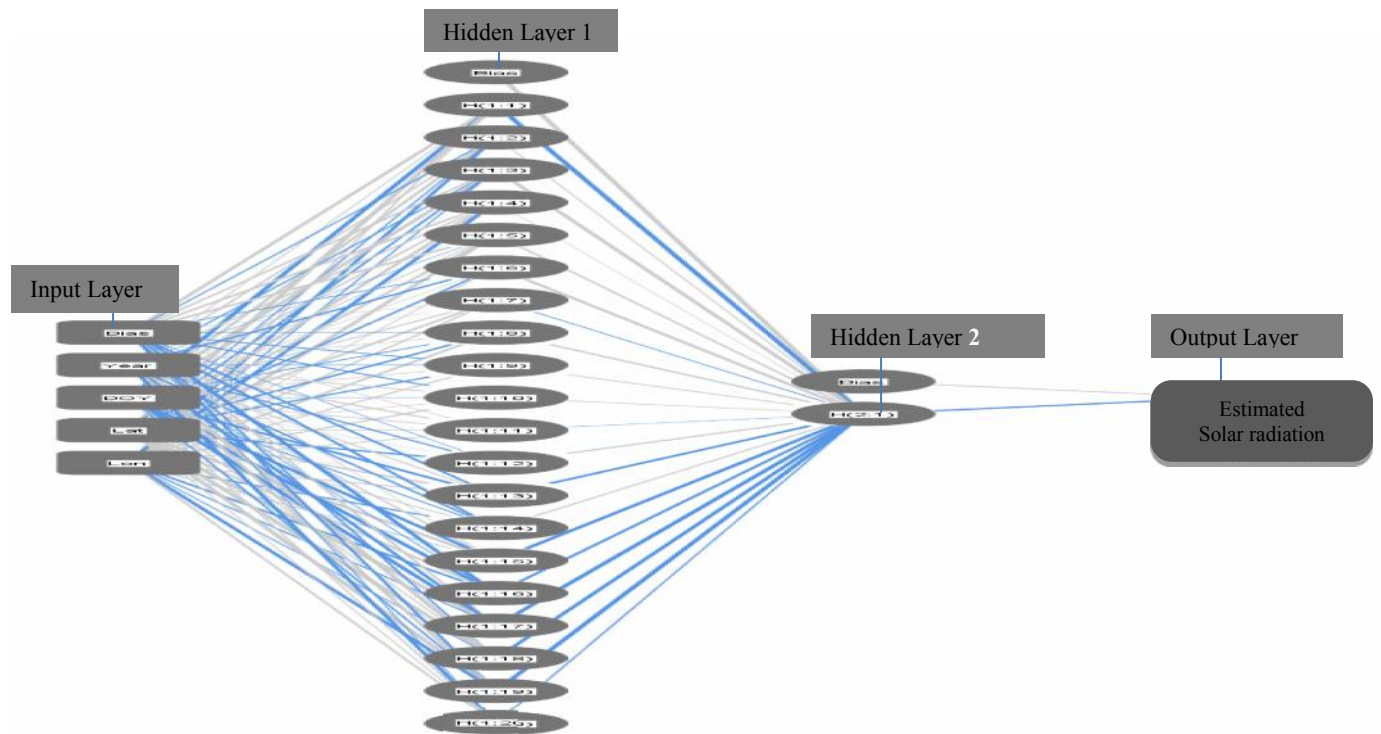
249



259 Figure 2: Feed-Forward Neural Network (FFNN) Three layers Model Training Setup Structure



261 Figure 3: Schematic Diagram of Neural Network Training window



262  
 263 Figure 2 showed that the size of  $l_{wm}$  is  $h$ -by-4 because there are 4 inputs layer neurons. The size  
 264 of  $L_{wm}$  is 1-by- $h$  because there is one output layer neuron. The sizes of  $b_1$ ,  $n_1$ ,  $H_{vm}$ ,  $b_2$  and  $n_2$   
 265 are  $h \times 1$ ,  $h \times 1$ ,  $h \times 1$ ,  $1 \times 1$  and  $1 \times 1$  respectively, where  $h$  is the number of hidden layer  
 266 neurons

267  
 268  
 269  
 270  
 271  
 272  
 273  
 274  
 275  
 276  
 277  
 278

279

280 **Figure 4: Network Diagram of the Model**

281 **2.2.5 Testing the Performances**

282 The performance function used to test the network of the data set after training before choosing  
283 the best network (net) is the mean square error (MSE) and root-mean-square-errors (RMSE)  
284 functions as given in equations (14) and (15).

285 
$$\text{MSE} = \frac{\sum (p - \text{obs})^2}{N} \quad 14$$

286 
$$\text{RMSE} = \sqrt{\frac{\sum (p - \text{obs})^2}{N}} \quad 15$$

287 where p and obs depict estimated and observed data, while N represent the total number of sample  
288 respectively.

289 **2.2.6 Using the network**

290 In this work, the best network obtained using the RMSE values at the end of the training was network  
291 (net) 16, that means at net 16 the best neural network model was observed. This best network model  
292 was used to determine the spatial distributions of solar radiation, estimate the daily values of solar  
293 radiation (temporal) and the annual average variations of the estimated and observed solar radiation. It  
294 was also used to forecast two-year (2018 and 2019) step ahead of daily solar radiation. It is pertinent  
295 to note that the model (net 16) has the ability of studying the distributions of solar radiation for each  
296 day from January to December across the years of study, but the month of January (1<sup>st</sup>) has taken to  
297 represents dry season, while the month of July (1<sup>st</sup>) was used to represent wet season for this study.  
298 This was done in order to also determine the seasonal variations of solar radiation in Nigeria.

299 **3. RESULTS AND DISCUSSION**

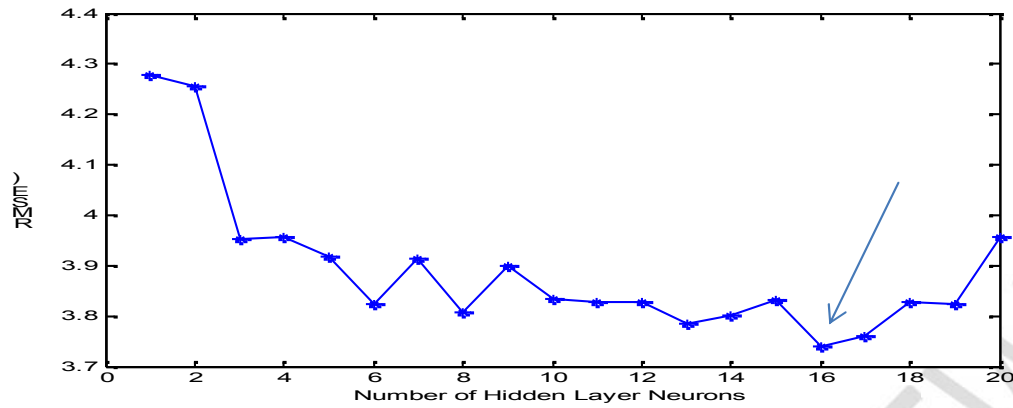
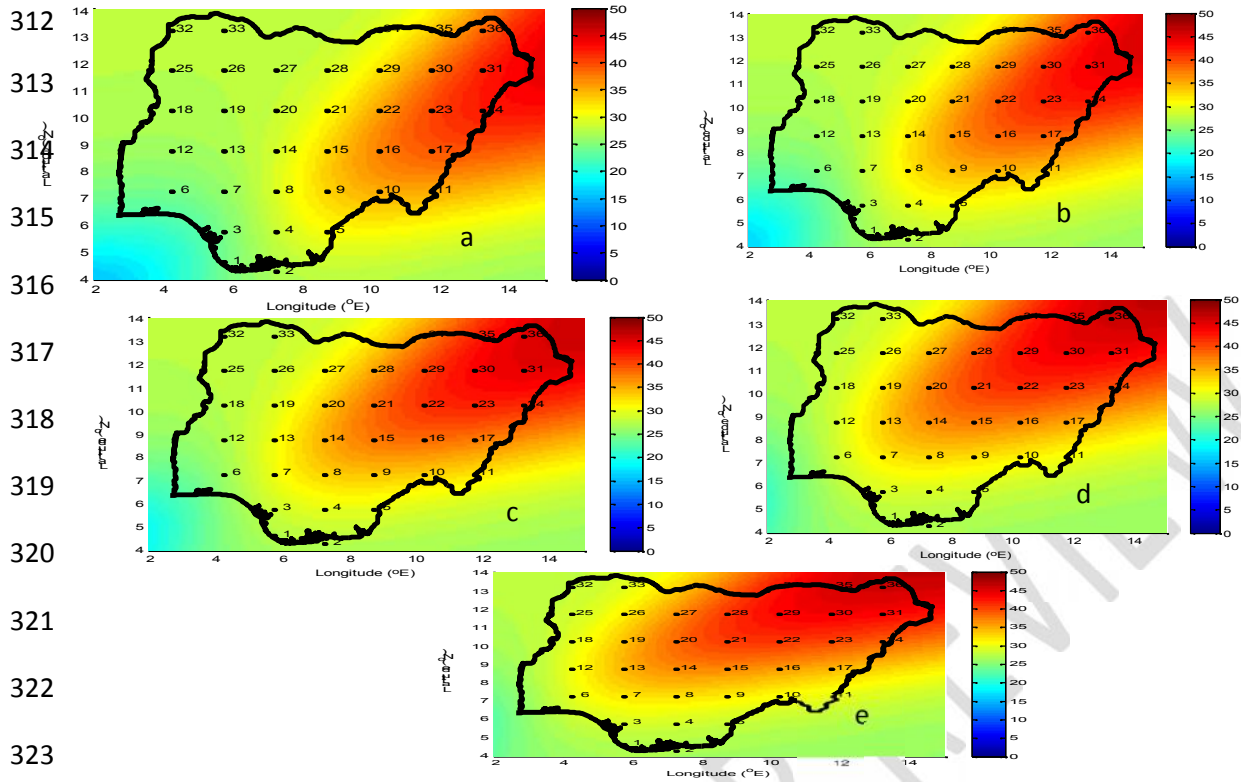


Figure 5

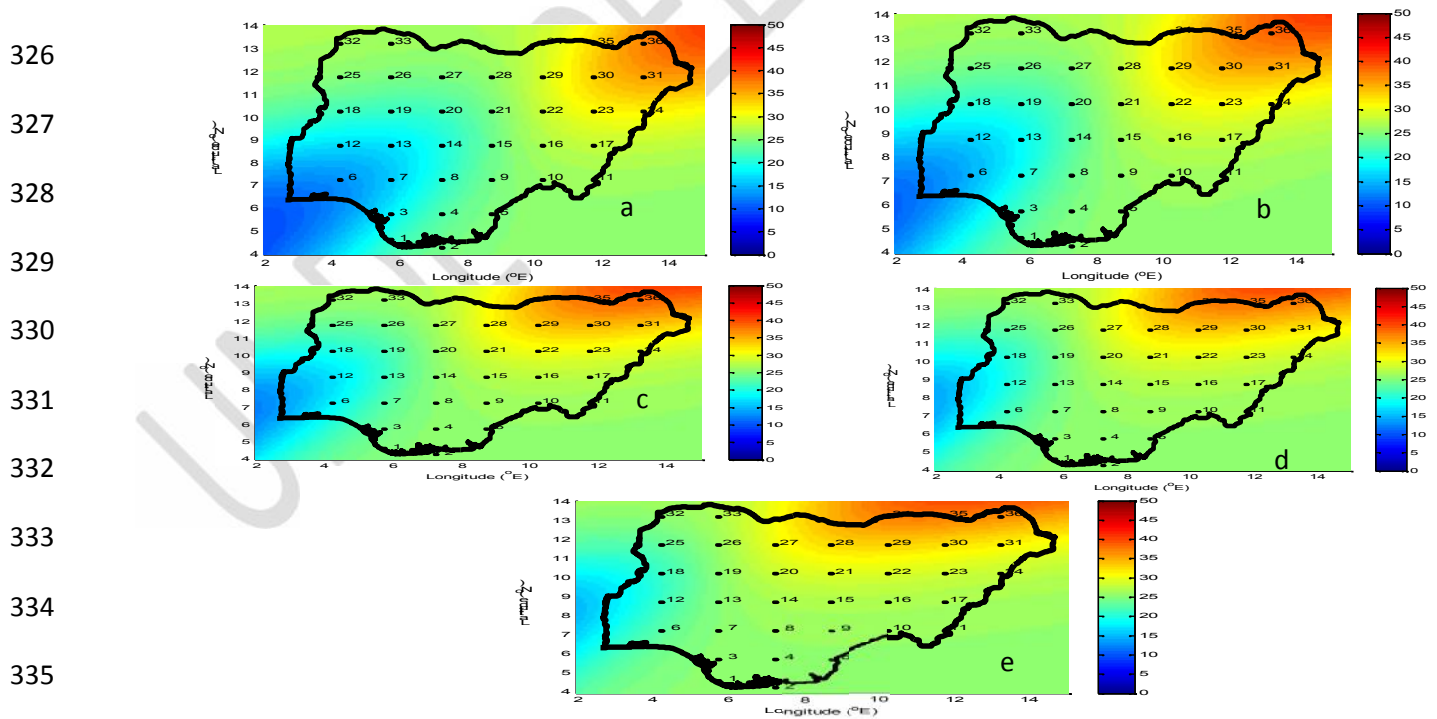
300  
 301 is the graph showing the relationship between RMSE and number of hidden layer neurons (1 to  
 302 20). The result reveals net 16 (indicated by a downward arrow) as the best network from the  
 303 training of solar radiation data.

304  
 305  
 306  
 307  
 308  
 309 **Figure 5:** Variations of the no of hidden layer neuron with root means square errors (rmse) of  
 310 solar radiation

311



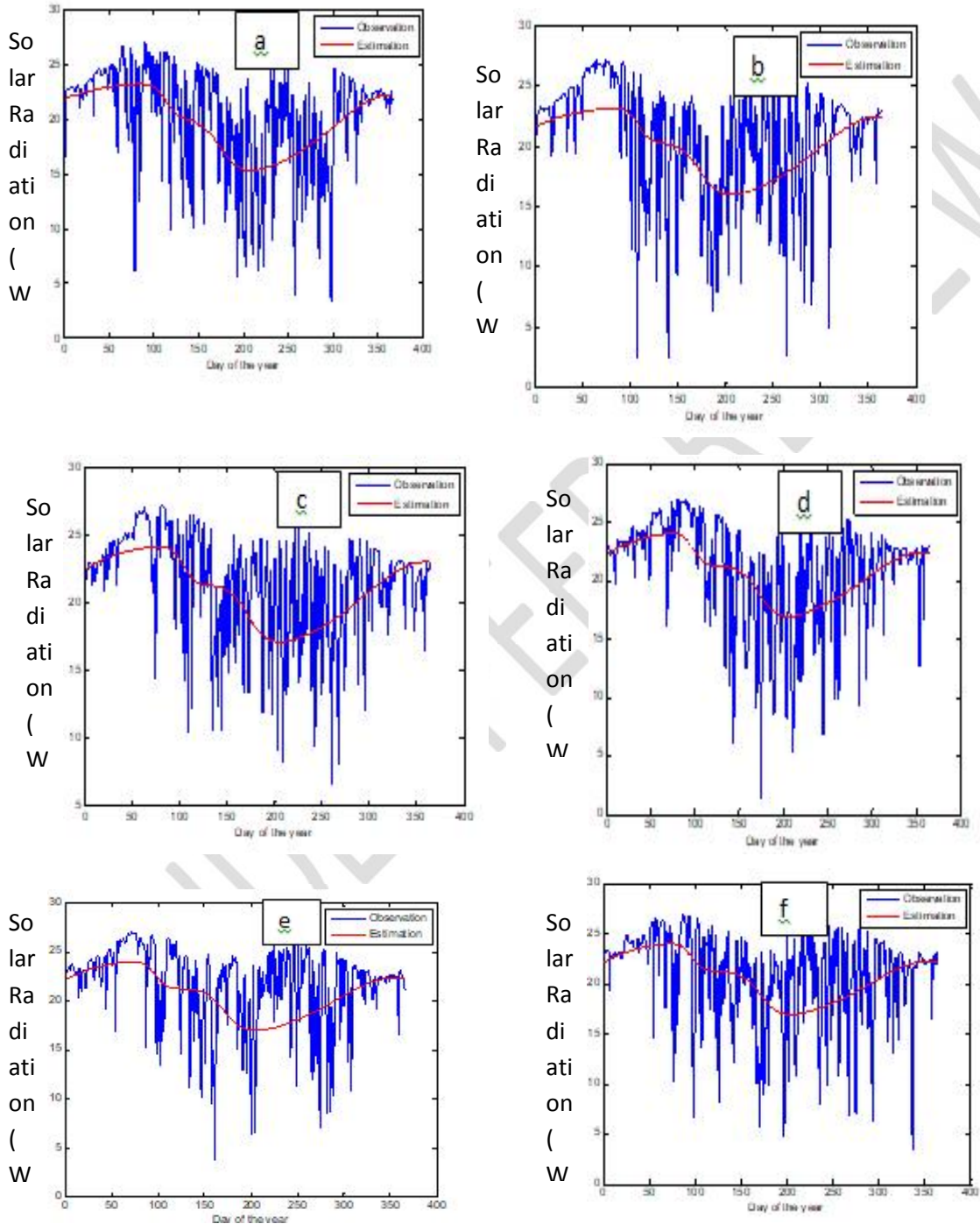
324 Figure 6: The spatial variations in solar radiation ( $w/m^2$ ) in dry season over Nigeria for the  
 325 periods: (a) 1979 (b) 1989 (c) 1999 (d) 2009 and (e) 2014.



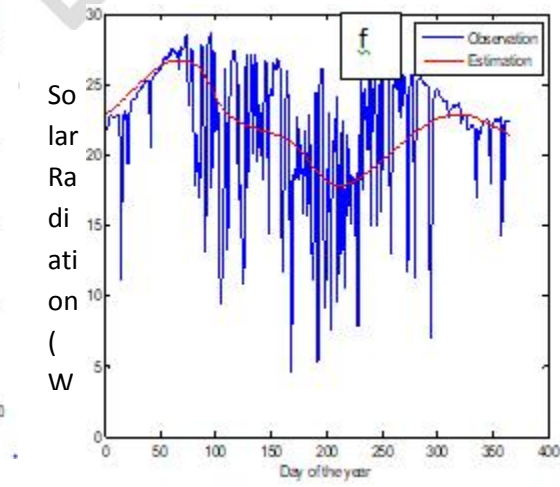
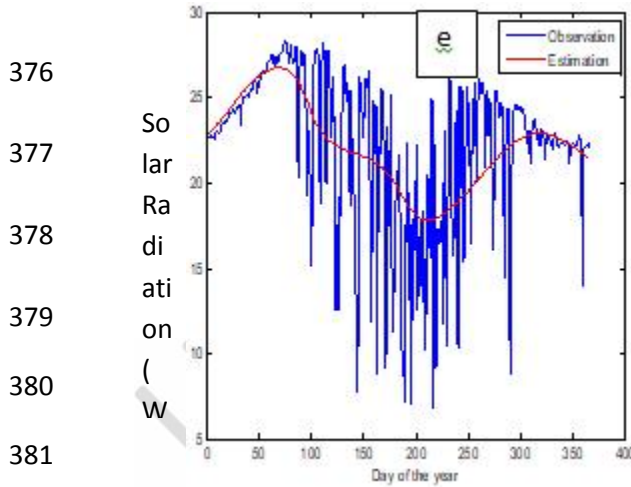
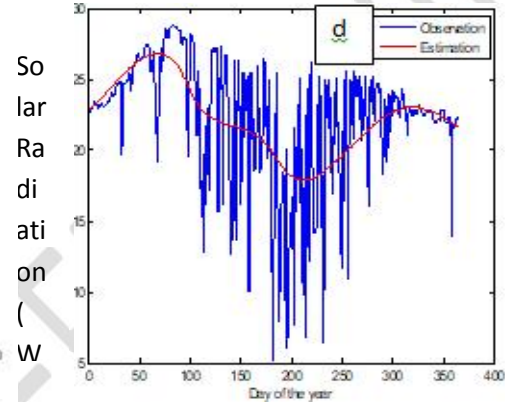
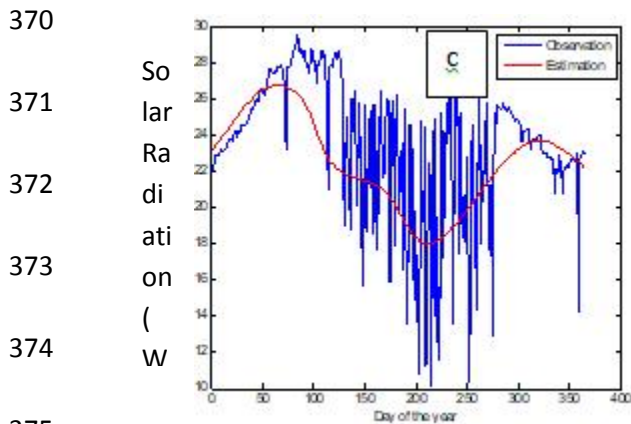
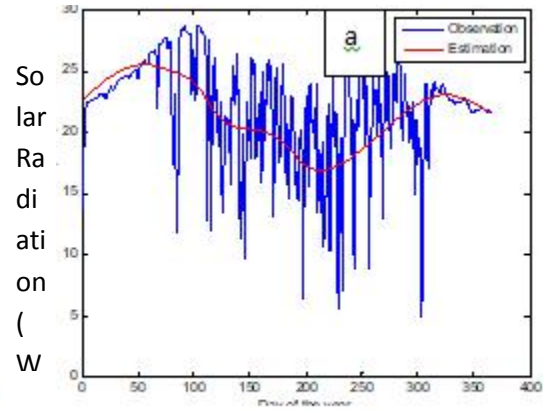
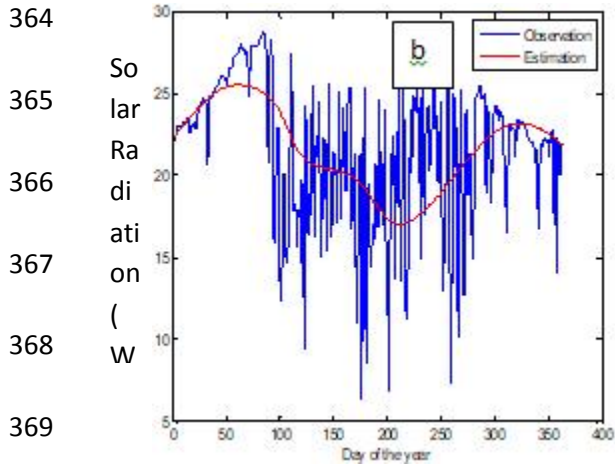
336 Figure 7: The spatial variations in solar radiation ( $w/m^2$ ) in wet season over Nigeria for the  
 337 periods: (a) 1979 (b) 1989 (c) 1999 (d) 2009 and (e) 2014



338  
339  
340  
341  
342  
343  
344  
345  
346  
347  
348  
349  
350  
351  
352  
353  
354  
355  
356  
357  
358  
359  
360  
361



362 Figure 8: The diurnal variations of observed and estimated solar radiation at Mowo, Osun State  
363 (4.25 °N: 7.25 °E) for the periods: (a) 1980 (b) 1990 (c) 2000 (d) 2010 (e) 2012 and (f) 2013.



382  
383

384 Figure 9: The temporal variations of solar radiation at Dindima, Bauchi State (10.25 °N: 10.25  
385 °E) for the periods: (a) 1980 (b) 1990 (c) 2000 (d) 2010 (e) 2012 and (f) 2013.

386



387

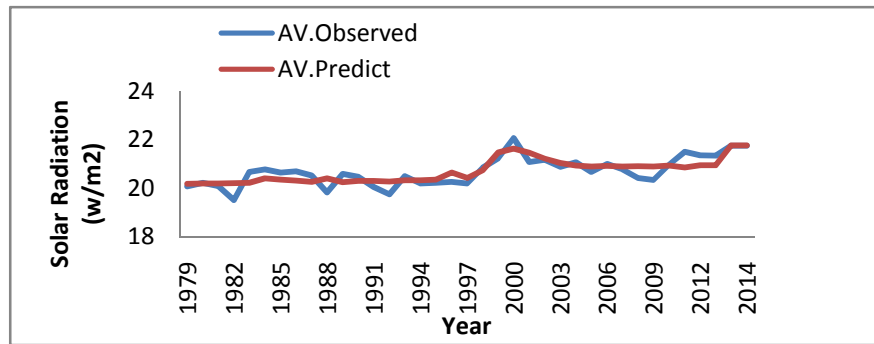
388

389

390

391

392



393 Figure 10: The Annual Average variations of estimated and observed values of solar radiation  
 394 (1979-2014)

395

396

397

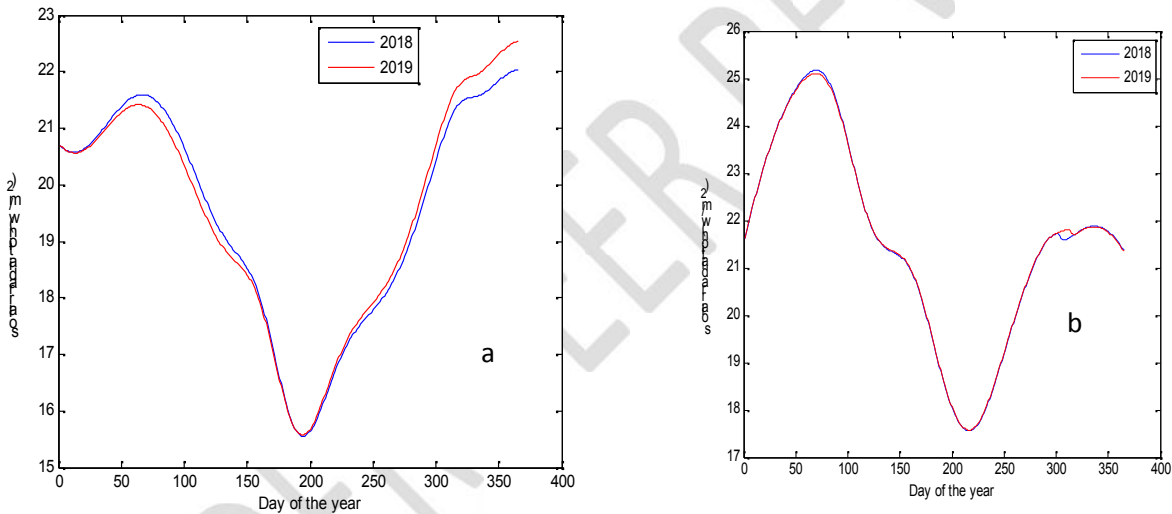
398

399

400

401

402



404 Figure 11: (a) Variations of forecast of 2018 and 2019 at Apoi Creek, Bayelsa State (4.59 °N: 5.84  
 405 °E) for solar radiation and (b) Variations of forecasts of 2018 and 2019 at Danjuma, Taraba State  
 406 (7.25 °N: 10.25 °E) for solar radiation

407 Data from thirty-six points over thirty-five years (1979-2014) were used to train, validate and  
 408 test the networks. The data from thirty-six points during learning and training were divided into  
 409 three portions randomly: 70% for the training, 15% for validation and the remaining 15% for  
 410 testing. Geographical parameters for these cities are given in Table 1, while location of the cities  
 411 on map is shown in Figure 1. The input parameters were year, day of the year, latitude and

412 longitude, while output parameter is the solar radiation. The observed data were also inputted as  
413 the targeted data. Artificial neural network topology used for the estimation of solar radiation is  
414 shown in Figure 3, while the network diagram of the training is shown in Figure 4. The drop  
415 down window at the end of the network training is shown in Figure 5. It was found that the most  
416 successful network (best network) was at layer network with 16 neurons in hidden layer.

417 Figure 6 (a – e) shows that the amount of solar radiation obtained in Nigeria between 1979 and  
418 2014 is in the range about 20 to 50 W/m<sup>2</sup>. The highest solar radiation of about 40 – 50 W/m<sup>2</sup>  
419 were obtained in the East and North-Eastern parts of Nigeria and the lowest of about 20-30 W/m<sup>2</sup>  
420 were obtained in the South-West and Southern parts of the country. From Figure 6 (a – e), it is  
421 observed that in dry season, between 1979 and 2014, the increase trends flow from North-East to  
422 North-West. This could be due to high intensity of solar irradiance in the Northern part of  
423 Nigeria particularly from Maiduguri (Borno State) as confirmed by [15, 16]. This could also be  
424 due to increase in the greenhouse gases as well as the gaseous pollutants due to high desert  
425 encroachment and human activities in the recent times over the region.

426 In Figure 7 (a – e), the result reveals that the spatial variations of solar radiation in wet season  
427 has the highest intensity of solar radiation at the North-Eastern part of the country from 1979 to  
428 2014. The locations with lowest amount of solar radiation 5 – 15W/m<sup>2</sup> increased drastically,  
429 while the locations with high amount (30 – 50 W/m<sup>2</sup>) reduced, especially in the North –Eastern  
430 part of Nigeria. It could be observed that within the periods under study, there was an increase in  
431 the number of points that received high intensities of solar radiation with more increase in the  
432 dry season than the wet season.

433 The comparison of solar radiation spatial variations during wet and dry seasons in Figures 6 and 7  
434 reveals that both of the seasons have their highest concentration in the North-East of Nigeria. It is  
435 pertinent to note that the lowest concentration occurred at North-West during wet season, while the  
436 lowest occurred at the South-South and South-West of Nigeria in dry season. In addition, the  
437 lowest in dry season is about 25 W/m<sup>2</sup>, while that of wet season is about 15 W/m<sup>2</sup>. Figures 8 and 9  
438 reveal that the signature of both the estimated and observed variations of solar radiation exhibit  
439 similar trends across the years of study. Hence the model exhibits good performance in estimating  
440 temporal solar radiation.

441 The coefficient of determination between the average yearly estimated and the observed solar  
442 radiation is 0.82, this imply 82% accuracies between the average yearly observed and estimated  
443 values. Figure 10 was further used to check the performance of the model. The graph indicates the  
444 annual patterns of flow of the global radiation for the period of 1979-2014; for both the real data  
445 and the simulated using neural network model. The graphs show how well the simulated data  
446 mimic the real data. The results show an excellent agreement between averages annually observed  
447 and estimated data. This observation indicates strong relation between the observed and estimated.  
448 It confirms high performance of the neural network model used for the estimation. This is in line  
449 with [17], which state that impressive performance of the neural networks model supports the  
450 application of neural network in modeling climatic parameters. Isikwue and Ibeh [18] also  
451 observed that neural network model performance were excellent and efficient in determination of  
452 spatial distribution of atmospheric parameters.

453 The model was used to predict daily data for two years steps (2018 and 2019) ahead the period of  
454 the study for two locations. One from the North, while the second from the South. In Figure 11 (a);  
455 solar radiation concentrations will be about 15.5-22.5 W/m<sup>2</sup>. The highest value of about 21- 22.5  
456 W/m<sup>2</sup> is predicted to be prevailing between January-March and October - December, while the  
457 small value of about 15.5 W/m<sup>2</sup> will be in June and July. This could be as a result of high dryness  
458 content in January-March and October – December, and high moisture content in June and July  
459 respectively. Observation shows that solar radiation decreases from day 60 – 180 (February-June),  
460 remain constant with about 15.5 W/m<sup>2</sup> between day 180 to 190 (July) before increasing again  
461 gradually to about 22.5 W/m<sup>2</sup> in day 365 (December). It is important to note that the result of the  
462 study reveals that solar radiation concentration will be lower in 2019 compared to 2018 between  
463 March to May, but will be higher in 2019 compared to 2018 between August and December. On  
464 the other hand, Figure 11b reveals the prediction of temporal distributions for two years steps  
465 ahead (2018 and 2019) for Danjuma, Taraba State, Northern part of Nigeria of solar radiation. The  
466 corresponding concentrations were between 15.5-25.5 w/m<sup>2</sup> respectively. It is important to note  
467 that the variation of the solar radiation in the South will be in variance with that of the North. Solar  
468 radiation concentration will be higher in the North. This could be as a result of Northern wind  
469 trade, proximity to Sahara desert and burning of fossil fuel in the region.

470

471

#### 472 4. CONCLUSION

473 Spatial distribution, temporal variations, annual distribution, estimation and prediction of solar  
474 radiations was carried out in this study using ANNs. Solar radiation data along the years (1979-  
475 2014) belonging to the thirty-six points in Nigeria were divided into three portions (training,  
476 testing and validation) during the applications of neural network model. The results of the  
477 validation and comparative study of the estimated and observed indicate that the ANN based  
478 estimation technique for solar radiation can be used to predict solar radiation as alternative to  
479 areas where in situ measurement cannot be possible in Nigeria. This study confirms the ability of  
480 the ANN models to predict solar radiation values precisely. The comparison results indicate that  
481 the ANN model is promising for evaluating the global solar radiation resource potential at the  
482 places where there are no monitoring stations in Nigeria.

#### 483 REFERENCE

- 484 1. Ibeh GF, Agbo GA, Agbo PE and Ali PA. Application of Artificial Neural Networks for  
485 Global Solar Radiation Forecasting With Temperature. *Advances in Applied Science*  
486 *Research*, 2012; 3 (1):130-134  
487
- 488 2. Tymvios FS, Jacovides CP, Michaelides SC and Scouteli C. Comparative study of  
489 Angstrom's and artificial network's methodologies in estimating global solar radiation,"  
490 *Solar Energy*. 2005;78(6): 752–762.  
491
- 492 3. Alawi SM and Hinai HA. An ANN-based approach for predicting global radiation in  
493 locations with no direct measurement instrumentation, *Renewable Energy*. 1998; 14:1–  
494 4,199–204.
- 495 4. Mohandes M, Rehman S, and Halawani TO. Estimation of global solar radiation using  
496 artificial neural networks. *Renewable Energy*. 1998; 14(1):179–184.
- 497 5. Mihalakakou G, Santamouris M and Asimakopoulos DN. The total solar radiation time  
498 series simulation in Athens, using neural networks," *Theoretical and Applied*  
499 *Climatology*, 2000; 66: 3-4, 185–197.
- 500 6. Reddy KS and Ranjan M. Solar resource estimation using artificial neural networks and  
501 comparison with other correlation models," *Energy Conversion and Management*. 2003;  
502 44(15):2519–2530.
- 503 7. Sozen A, Ozalp M, Arcaklioglu E and Kanit EG. A study for estimating solar resource in  
504 Turkey using artificial neural networks," *Energy Sources*, 2004; 26: 1369–1378.
- 505 8. Mubiru J and Banda EJKB. Estimation of monthly average daily global solar irradiation  
506 using artificial neural networks. *Solar Energy*. 2008; 82(2):181–187.
- 507 9. Demuth H and Beale M. *Neural Network Toolbox for use with MATLAB*. The  
508 Mathworks Incorporation: Natick, MA. 2002; 01760-2098

509 10. Kisi O and Uncuoglu E. Comparison of three back-propagation training algorithms for  
510 two case studies. *Indian Journal of Engineering and Material Science*. 2005; 12: 434–  
511 442.

512 11. Buhari M and Adamu SS. Short-Term Load Forecasting using Artificial Neural Network.  
513 *Proceedings of the International Multi-Conference of Engineers and Computer Scientists*  
514 *IMECS, Hong Kong*. 2012; pp 4-23.

515 12. Sheela KG and Deepa SN. A new algorithm to find number of hidden neurons in Radial  
516 Basis Function Networks for wind speed prediction in renewable energy systems. *Control*  
517 *Engineering Application Information*. 2013; 15(3): 30-37

518 13. Dong X, Beijing L and Yachun M. A Multiple Hidden Layers Extreme Learning  
519 Machine Method and Its Application. *Mathematical Problems in Engineering*. 2017;  
520 2017: 1-10

521 14. Beale MH, Haagan MT and Demuth BH. *Neural Network Toolbox™. User's Guide*  
522 *(R2015a)*. The Math Works, Incorporation. 2015; Pp 10- 20

523 15. Osueke CO, Uzendu P and Ogbonna ID. Study and Evaluation of Solar Energy Variation  
524 in Nigeria. *International Journal of Emerging Technology and Advanced Engineering*.  
525 2013; 3(6): 501-506

526 16. Olaide MA, Guerner AD and Zhou E. Assessment of Renewable Energy Sources and  
527 Municipal Solid Waste for Sustainable Power Generation in Nigeria. *Earth and*  
528 *Environmental Science*.2017; 95: 1-10

529 17. Daniel O, Najib Y, Oluwaseye A, Ibrahim M and Bababtunde R. Preliminary results  
530 of temperature modeling in Nigeria using neural networks. *Royal Meteorological*  
531 *Society*. 2015; 70:336-342.

532 18. Isikwue BC and Ibeh GF. Investigation of Carbon Dioxide Variations in Selected Points  
533 in Nigeria Using Neural Network Model *Asian Journal of Environment & Ecology* 2019;  
534 9(1): 1-11  
535  
536  
537